Volume 15, Issue 4, 152428 (1-11)

International Journal of Nano Dimension (IJND)

https://dx.doi.org/10.57647/j.ijnd.2024.1504.28

Synthesis of copper and cobalt oxide nanoparticles for enhanced supercapacitor applications

Damodaram Vandana Reddy[1], Chindukuri Maneesha[1], Lakshmana Naik Ramavathu[2,*], Tumma Bala Narasaiah[1]

[1]*Jawaharlal Nehru Technological University Anantapur, Ananthapuramu, Andhra Pradesh, India.*
[2]*Indian Institute of Technology Jodhpur, Karwar, Jodhpur, Rajasthan, India.*

[*]**Corresponding author:** lakshman2027@gmail.com

Original Research

Received:
14 February 2024
Revised:
25 June 2024
Accepted:
29 June 2024
Published online:
10 October 2024

Abstract:

This research paper presents a comprehensive study on the synthesis of copper oxide (CuO), cobalt oxide (Co_3O_4), and their hybrid nanoparticles via the sol-gel method for enhanced supercapacitor applications. The resulting materials were characterized using techniques such as X-ray diffraction (XRD), scanning electron microscopy (SEM), UV-Vis, Dynamic Light Scattering (DLS) and electrochemical measurements. The average particle size of CuO, Co_3O_4 nanoparticles and CuO/Co_3O_4 nanocomposite is found from XRD as 18.5 nm, 18.1 nm, and 17.5 nm respectively. The electrochemical performance of the synthesized nanoparticles was evaluated using cyclic voltammetry (CV). The CuO nanoparticles exhibited a specific capacitance of 204 F/g, while Co_3O_4 showed a specific capacitance of 252 F/g at a scan rate of 5 mV/s. The CuO-Co_3O_4 hybrid nanoparticles demonstrated a synergistic effect, with a specific capacitance of 384 F/g, outperforming the individual oxide counterparts.

Keywords: Cobalt oxide; Cooper oxide; Sol-gel method; Specific capacitance; Supercapacitor

1. Introduction

In recent years, there has been a growing interest in finding effective energy storage solutions because to the increasing need for portable gadgets, electric cars, and the integration of renewable energy into the power grid [1, 2]. The emergence of supercapacitors as energy storage devices has garnered significant attention due to its capacity to provide high power densities, rapid charge-discharge rates, and extended cycle lifetimes, thereby serving as a valuable complement to conventional battery technologies [3, 4]. The electrode materials for supercapacitors have attracted significant interest due to the high specific capacitance, chemical stability, and environmental compatibility exhibited by transition metal oxides [5, 6]. Among these transition metal oxides, copper oxide (CuO) and cobalt oxide (Co_3O_4) stand out as promising candidates for supercapacitor applications due to their excellent electrochemical properties [7, 8]. Their redox reactions, high theoretical capacitances, and abundance make them appealing choices for enhancing the performance of energy storage devices.

Copper and cobalt oxides find diverse applications in various fields, serving as pivotal materials in modern research endeavours [9]. In the realm of energy storage, copper oxide emerges as a promising candidate for supercapacitors, owing to its high specific capacitance and excellent cycling stability. Its application extends to catalysis, where cobalt oxide nanoparticles exhibit remarkable efficiency in water oxidation reactions [10], crucial for sustainable energy production through water splitting [11]. Moreover, in the realm of biomedical research, cobalt oxide nanoparticles show potential as contrast agents in magnetic resonance imaging (MRI) due to their magnetic properties, offering non-invasive and highly sensitive imaging modalities for disease diagnostics [12]. These multifaceted applications underscore the pivotal roles of copper and cobalt oxides in advancing diverse fields of scientific exploration and technological innovation. Copper oxide, in its various forms including CuO and Cu_2O, exhibits a rich redox behaviour that enables reversible Faradaic reactions, leading to high specific capacitance values [13, 14]. Its layered crystal

structure allows for facile ion diffusion, facilitating rapid charge and discharge processes essential for efficient energy storage. Moreover, the abundance and eco-friendliness of copper oxide make it an attractive choice for sustainable energy applications.

On the other hand, cobalt oxide, particularly in its Co_3O_4 spinel form, presents a unique electrochemical profile characterized by multiple redox couples [15]. This feature results in a high pseudocapacitance contribution, leading to enhanced energy storage capabilities. Additionally, cobalt oxide demonstrates excellent conductivity and stability, ensuring prolonged cycling performance for pseudocapacitor devices. In recent years, the integration of these transition metal oxides into hybrid structures has emerged as a strategy to further enhance the electrochemical performance of pseudocapacitors [16, 17].

Hybrid nanoparticles combining copper oxide and cobalt oxide (CuO/Co_3O_4) offer synergistic effects, such as improved charge transfer kinetics, enhanced specific surface area, and optimized ion diffusion pathways [18, 19]. These features collectively contribute to the superior electrochemical properties of the resulting electrodes, making them highly desirable for next-generation energy storage applications [20–22]. Furthermore, the synthesis of these metal oxides into nanostructured forms offers additional advantages such as increased surface area, improved electronic conductivity, and enhanced electrochemical reactivity [23–25]. Copper oxide (CuO) is considered environmentally benign due to its non-toxic nature and minimal environmental impact during disposal. The widespread availability and relatively low cost of copper make CuO an economically attractive material for supercapacitors. Its low cost combined with good electrochemical performance offers a favourable cost-to-performance ratio.

Nanomaterials can be utilized for energy storage through two methods: direct and indirect. The materials are composed of porous materials with a significant surface area, enabling the storage of electric charges through electrostatic adsorption on the surface and pores [26, 27]. The material charge storage occurs by quick faradic reactions at the interface between the electrode and electrolyte, resulting in a phenomenon known as pseudocapacitance [28–31]. Pseudocapacitors, such as RuO_2, MnO_2, Co_3O_4, Fe_2O_3, CuO, and NiO, exhibit a diverse spectrum of particle sizes and morphologies, enabling them to effectively store charge [32–36]. Therefore, metal oxides are essential to explore its understanding in great details in terms of their synthesis, properties and applications.

This manuscript presents a systematic investigation into the synthesis of CuO and Co_3O_4 and their hybrid nanoparticles (CuO/Co_3O_4) using the sol-gel method for application in supercapacitors. The sol-gel method used in our synthesis is known for its low energy requirements and minimal environmental footprint compared to other high-temperature processes. The process also allows for the precise control of material properties, reducing waste and improving efficiency. The sol-gel method offers precise control over nanoparticle size, morphology, and composition, making it an attractive approach for tailoring electrode materials with desired properties [37]. In our study, we selected copper chloride dihydrate ($CuCl_2{\cdot}2H_2O$) and cobalt chloride hexahydrate ($CoCl_2{\cdot}6H_2O$) as the precursors for the synthesis of copper oxide (CuO) and cobalt oxide (Co_3O_4) nanoparticles, respectively. These precursors were chosen due to their high solubility in the reaction medium, ease of handling, and their effectiveness in forming homogeneous gels. The concentrations of the precursors were optimized through preliminary experiments to ensure a balanced stoichiometric ratio conducive to the formation of CuO, Co_3O_4, and their hybrid nanoparticles with desired purity and crystallinity. By combining copper oxide, cobalt oxide, and their hybrids, this study aims to explore the synergistic effects that can potentially enhance the electrochemical performance of supercapacitors. Understanding the intricacies of synthesizing copper oxide, cobalt oxide, and their hybrid nanoparticles via the sol-gel method is crucial for optimizing their performance as supercapacitor electrodes. This work attempts to add to the increasing amount of information in this area by offering insights into the development, synthesis, and characterisation of sophisticated electrode materials suited for high-efficiency supercapacitor applications. The objective of this study is to establish a foundation for the advancement of energy storage devices in the future, characterized by enhanced efficiency, reliability, and environmental sustainability.

2. Materials and methods

2.1 Materials

For the synthesis of copper oxide (CuO) nanoparticles, cobalt oxide (Co_3O_4) nanoparticles, and copper oxide/-cobalt oxide (CuO/Co_3O_4) composite following chemicals are used. Copper chloride dihydrate ($CuCl_2{\cdot}2H_2O$), Cobalt chloride hexahydrate ($CoCl_2{\cdot}6H_2O$), Copper sulphate pentahydrate ($CuSO_4{\cdot}5H_2O$), Sodium hydroxide pellets (NaOH), Sodium carbonate (Na_2CO_3), Hexa methylene tetra amine ($(CH_2)_6N_4$), Ammonium bicarbonate (NH_4HCO_3), Hydrochloric acid (HCl) and Distilled water (H_2O).

2.2 Synthesis of nanoparticles

The nanoparticles were synthesized through the utilization of a wet chemical (Sol-Gel) technique. This technique involves dissolving the molecular precursor in water and transforming it into a gel by the process of hydrolysis, which is achieved by heating and stirring.

2.2.1 Copper oxide (CuO) nanoparticles

For the preparation of CuO nanoparticles, 0.51 g of copper chloride dihydrate ($CuCl_2{\cdot}2H_2O$) was dissolved in 100 mL of distilled water. The reaction mixture was stirred and heated to 50 °C for a period of 1 hour. At the time of vigorous stirring, add 1 g of NaOH pellets to the solution. Then the colour of the solution turns from blue colour to green colour and finally black colour homogeneous precipitate was obtained. Then, add few drops of hydrochloric acid (HCl) to adjust the pH of the solution. This black colour precipitate is copper hydroxide.

2.2.2 Cobalt oxide (Co_3O_4) nanoparticles

For the preparation of Co_3O_4 particles, add 1 g of cobalt chloride hexahydrate ($CoCl_2 \cdot 6H_2O$) and sodium carbonate (Na_2CO_3) in 100 mL distilled water in a 250 mL conical flask. Under the vigorous stirring for an hour, the colour of the solution turns to violet colour precipitate. Here cobalt chloride hexahydrate acts as a precursor and sodium carbonate acts as a reducing agent.

2.2.3 Copper oxide/Cobalt oxide (CuO/Co_3O_4) composite

For the synthesis of the copper oxide/cobalt oxide nanocomposite by using precursors of each 10 mmol of copper sulphate pentahydrate ($CuSO_4 \cdot 5H_2O$), and cobalt chloride hexahydrate ($CoCl_2 \cdot 6H_2O$) in a 40 mL distilled water in a conical flask. To this solution reducing agents of 20 mmol of hexamethylenetetramine ($(CH_2)_6N_4$), and 15 mmol of ammonium bicarbonate (NH_4HCO_3) in 40 mL distilled water was added dropwise under vigorous stirring and heating up to 50 °C for 1 h. The colour of the solution changes from maroon to lavender and then malachite blue.

The homogeneous precipitate obtained from the above procedures was filtered by centrifuge and then washed with distilled water several times to remove the impurity ions. The resulting gels were dried in an oven at 70 °C for 4 hours to remove any residual solvents and to obtain xerogels. The dried xerogels were subjected to calcination in a muffle furnace. The dried nanoparticles (CuO, Co_3O_4 CuO/Co_3O_4) were calcined at 450 °C for 3 hrs to achieve optimal phase formation and crystallinity. After calcination, the samples were allowed to cool to room temperature naturally. The nanoparticles were finely ground into fine powers using an agate mortar and pestle to ensure uniform particle size distribution of CuO, Co_3O_4, CuO/Co_3O_4 nanoparticles.

2.3 Characterization

A Shimadzu x-ray diffractometer PANALYTICAL XPERT'[3] PRO was used to study the crystalline features of the sample in the 2θ range from 20–80°. Fourier Transform Infrared (FTIR) spectroscopy was performed using a Bruker ALPHA II - Eco FT-IR with a Diamond Crystal ATR Spectrometer. UV-Visible (UV-vis) studies were conducted using a Double Beam UV-VIS Spectrophotometer (Model No. HV-2201) in the range from 200–800 nm. Nanopartica SZ-100 is used for measuring the size distribution of particles.

1 mg of each active material (CuO, Co_3O_4 nanoparticles & CuO, Co_3O_4 nanocomposite) was combined with 5 µL of Nafion and a small amount of ethanol solution for the purpose of electrochemical analysis. The solution was sonicated for 1 hour in order to achieve a homogeneous slurry. Subsequently, this slurry was applied onto a glassy carbon electrode (GCE) with an area of 1 cm^2 and left to dry at room temperature. A three-electrode system has been used to do electrochemical analysis, with the active material functioning as the working electrode, a platinum wire serving as the counter electrode, and Ag/AgCl being employed as the reference electrode. Furthermore, a solution of potassium hydroxide (KOH) with a concentration of 1 M was employed as the electrolyte. The active material electrode was subjected to cyclic voltammetry study at different scan rates spanning a potential range of 0.0 to 0.6.

3. Results and discussion

3.1 X-ray diffraction (XRD) analysis

The XRD analysis of synthesized CuO, Co_3O_4, CuO/Co_3O_4 nanoparticles, was identified and shown in figure 1. The intense peaks at 2θ values of 32.6° (110), 35.6° (111), 36.9°

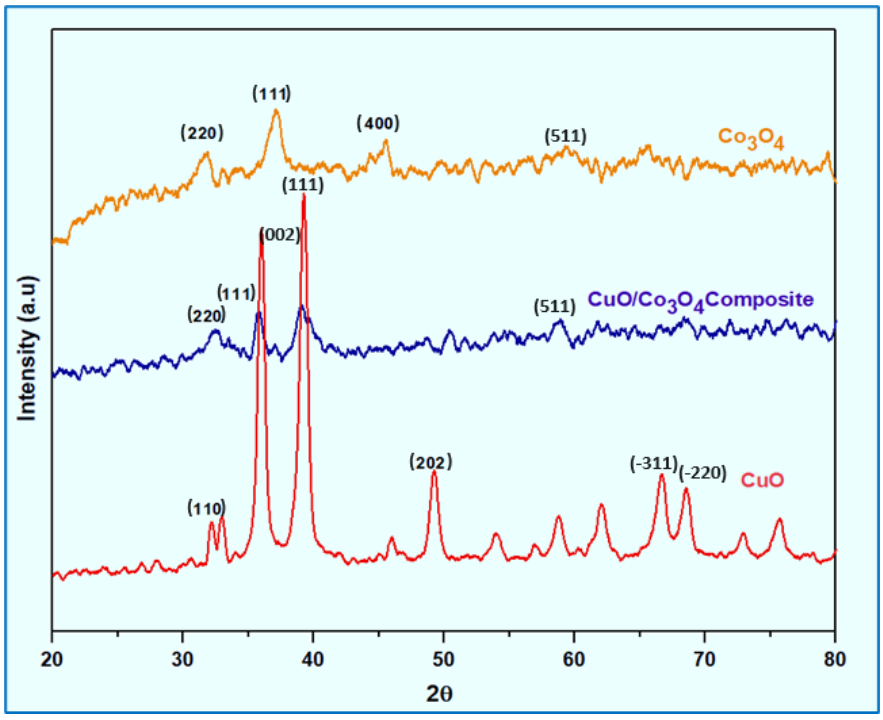

Figure 1. XRD analysis of CuO, Co_3O_4 nanoparticles and CuO/Co_3O_4 nanocomposite.

(111), 38.8° (111), 44.9° (202), 66.2° (-311) and 68.3° (-220) corresponding to the crystal structure of monoclinic tenorite for CuO nanoparticles, normal spinel structure for Co_3O_4 nanoparticles and cubic structure for CuO/Co_3O_4 composite. These values are matching with JCPDS No.01-080-1916 (CuO) and 00-073-1701 (Co_3O_4). The average particle size of CuO, Co_3O_4 nanoparticles and CuO/Co_3O_4 nanocomposite was estimated by using Debye Scherrer formula which is found at 18.5 nm, 18.1 nm, and 17.5 nm respectively.

The XRD graph is plotted against diffracted intensity vs 2θ. The crystalline size of samples estimated from the most intense peak of XRD pattern using Debye Scherer's formula [38].

$$D = \frac{0.9\lambda}{\beta \cos\theta} \quad (1)$$

where λ = wavelength of X-rays (1.54 nm for Cu), β = full width half maxima of a peak, θ = angle of the peak.

3.2 Scanning electron microscopy (SEM) and EDAX analysis

The surface morphology of synthesized materials is analysed by using SEM as shown in figure 2(a-c). FESEM image of CuO nanoparticle as shown in figure 2(a) are having flake-like structure, SEM image of Co_3O_4 nanoparticle shown in figure 2(b,c) and composite (CuO/Co_3O_4) are in agglomerated with irregular shape.

The energy dispersive X-ray spectroscopic technique was employed to observe the elemental composition of the produced nanomaterials, as represented in figure 2(d), 2(e) and 2(f). This EDAX confirms the presence of Cu and O for CuO nanoparticle sample, Co and O for Co_3O_4 nanoparticle and the combination of Cu, Co, O for composite material.

3.3 Particle size distribution

Dynamic Light Scattering (DLS) technique measures size distribution of nanoparticles. The DLS data provided information on the hydrodynamic diameter of the nanoparticles, offering insight into the size distribution and the degree of agglomeration in the samples. The particle size distribution of CuO, Co_3O_4 nanoparticles and their composite (CuO/Co_3O_4) are having diameter range 1–10 nm, 10–100 nm, and 10–100 nm as determine on laser light scattering particle size analyser which are shown in figure 3(a-c). From the results of DLS it is observed that the particles are well dispersed. For CuO nanoparticles, the DLS analysis

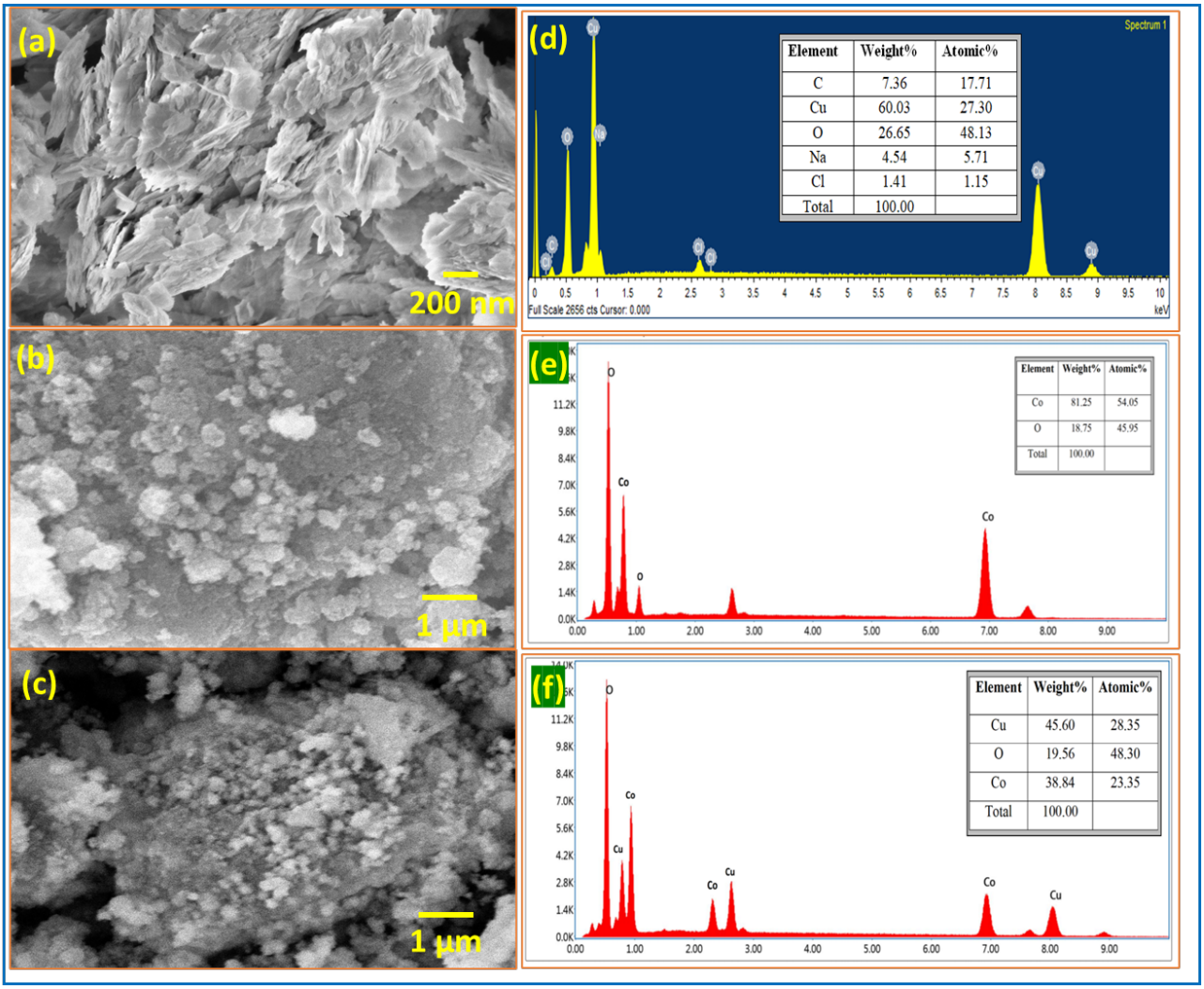

Figure 2. (a,b,c) SEM images, (d,e,f) EDAX image of CuO, Co_3O_4 and CuO/Co_3O_4 nanocomposite.

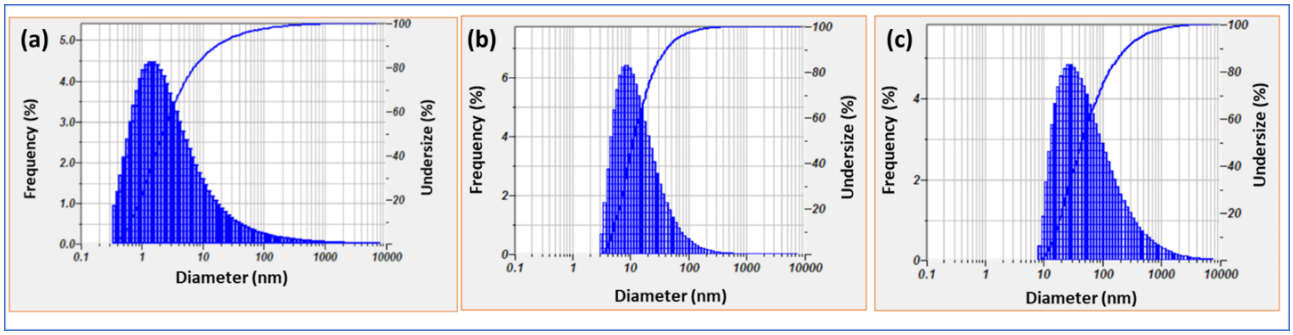

Figure 3. (a) DLS graph of CuO nanoparticle, (b) Co_3O_4 nanoparticle, (c) CuO/Co_3O_4 nanocomposite.

as shown in figure 3(a) revealed a mean particle size of approximately 10 nm with a relatively narrow size distribution, indicating good uniformity. For Co_3O_4 nanoparticles, the DLS results showed a mean particle size of approximately 22 nm, with a broader distribution, suggesting some degree of agglomeration. For the hybrid CuO-Co_3O_4 nanoparticles, the DLS analysis indicated a mean particle size of approximately 40 nm, with a uniform size distribution profile of the metal oxides.

3.4 Fourier transform infrared spectroscopy (FI-TR) analysis

The functional groups present in the synthesized materials are found from FTIR analysis shown in figure 4(a-c). The peaks at 660.9 cm^{-1}, 689.9 cm^{-1}, 749.97 cm^{-1} have strong absorption band corresponds to Cu-O stretching bond, Co-O bond due to the presence of CuO in monoclinic phase and Co_3O_4 in spinel phase [39]. The broad band centred in the region 3435.5 cm^{-1}, 3423.05 cm^{-1}, 3445.9 cm^{-1} is allocated to the bending vibrations of surface hydroxyls [40]. Similarly, C-H stretching bonds occur in the region 3100–2800 cm^{-1}. The peaks obtained at 1625.5 cm^{-1}, 1634.1 cm^{-1}, 1631.4 cm^{-1} indicates C=O stretching bonds.

3.5 UV-visible analysis

The UV-Vis absorbance spectrum (wavelength vs absorbance) of synthesized materials is used to study the band gap energy and electronic transitions of certain material. The absorption spectra of CuO, Co_3O_4 nanoparticle and CuO/Co_3O_4 composite were shown in below figure 5(a-c). The energy band gap of the obtained CuO, Co_3O_4 nanoparticle and CuO/Co_3O_4 nanocomposite are 2.4 eV, 2.2 eV and 1.9 eV respectively as shown in figure 5(d-f) is determined

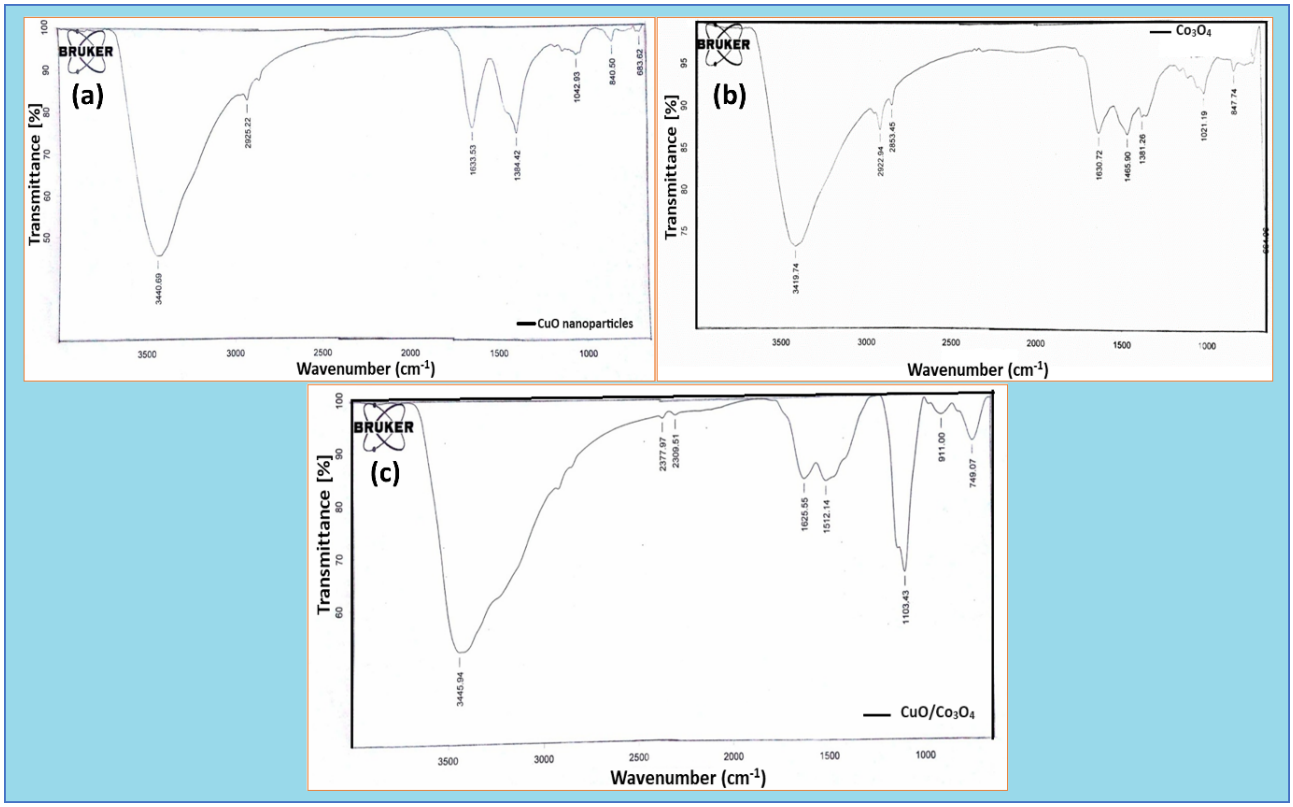

Figure 4. FTIR spectra of (a) CuO, (b) Co_3O_4 nanoparticles, (c) CuO/Co_3O_4 nanocomposite.

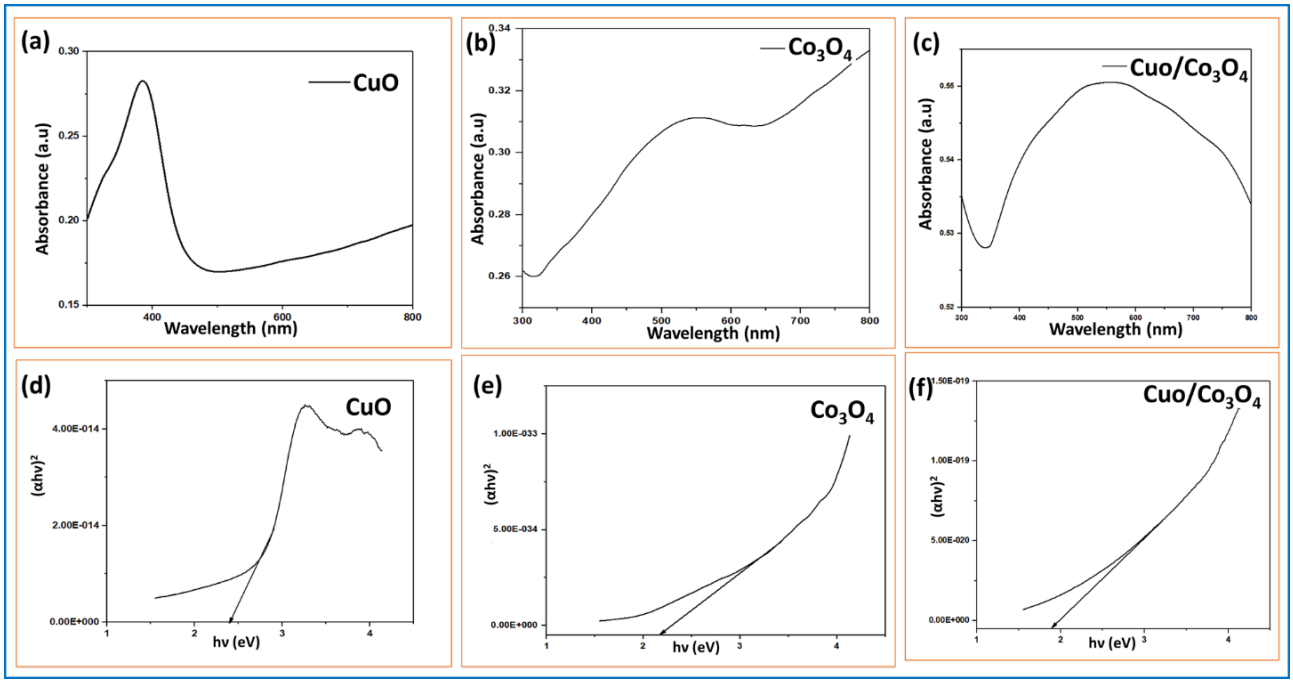

Figure 5. (a-c) UV-Vis absorption spectra of CuO, Co_3O_4 and CuO/Co_3O_4 nanocomposite, (d-f) Tauc plot of direct electronic transition of CuO, Co_3O_4 and CuO/Co_3O_4 nanocomposite.

by using Tauc's relation [41].

$$(\alpha h\vartheta)^n = \mathrm{A}(h\vartheta - E_g) \tag{2}$$

where α = absorption coefficient, $h\vartheta$ = incident photon energy, A = material dependent constant, n = 2 for direct transitions, n = ½ for indirect transitions and E_g = energy band gap. Using this relation Tauc plot is drawn for direct and indirect allowed electronic transitions of CuO, Co_3O_4 nanoparticle and CuO/Co_3O_4 composite. This tauc plot represents the relationship between photon energy vs $(\alpha h)^n$. The obtained graphs for direct transitions are seen in figure 5(a,d) of CuO nanoparticles, figure 5(b,e) Co_3O_4 nanoparticle and figure 5(c,f) of CuO/Co_3O_4 nanocomposite.

3.6 Electrochemical analysis (cyclic voltammetry (CV) analysis)

The cyclic voltagram of CuO, Co_3O_4 nanoparticles, and CuO/Co_3O_4 nanocomposite with varying scan rates at a potential range of 0.0 to 0.6 V, employing 1 M KOH as the electrolyte, is displayed in figure 6(a-c). The shape of CV curve of samples confirms the presence of redox peaks in their cathodic and anodic peak current density within the different scan rates and indicates clearly that these nanomaterials having pseudocapacitive characteristics [42]. The CV curve exhibits a shape that is approximately rectangular, providing evidence for the faradic nature of the materials. The below formula [43] is used to compute the maximum specific capacitance of nanomaterials.

$$C = \frac{Q}{m \cdot \Delta V} \tag{3}$$

In this context, C represents the specific capacitance, Q denotes the average charge observed throughout both the anodic and cathodic scans, m signifies the mass of the active material, and ΔV represents the applied potential range.

CuO and Co_3O_4 each exhibit pseudocapacitive behaviour, where charge storage occurs through redox reactions. The hybrid structure benefits from the combined pseudocapacitive effects of CuO (Cu^{2+} to Cu^{3+} and Cu^{+} transitions) and Co_3O_4 (Co^{3+} to Co^{4+} transitions), enhancing the overall capacitance. The interface between CuO and Co_3O_4 creates unique electronic environments, facilitating efficient charge transfer and reducing the charge transfer resistance. This synergy enhances the electrochemical reaction kinetics, contributing to higher specific capacitance.

The synergistic effect in CuO-Co_3O_4 hybrid nanoparticles likely arises from several factors that enhance their overall electrochemical performance compared to the individual components. CuO and Co_3O_4 have different electrochemical behaviours that complement each other. CuO provides high specific capacitance due to its pseudocapacitive nature, while Co_3O_4 offers excellent electrical conductivity and stability. The combination of these properties results in a material that benefits from both high capacitance and good conductivity. The hybrid structure facilitates efficient electron and ion transport. The Co_3O_4 matrix can provide a conductive network that improves electron mobility, while the dispersed CuO nanoparticles ensure ample electroactive sites for ion storage. This dual network enhances the overall charge storage and transfer efficiency. The incorporation of CuO into the Co_3O_4 matrix can improve the structural stability of the composite material. The hybrid nanoparticles often exhibit a higher surface area compared to individual oxides, providing more active sites for electrochemical reactions and improving capacitance.

The maximum specific capacitance of these materials with different scan rates is plotted in figure 6(d) and shown in

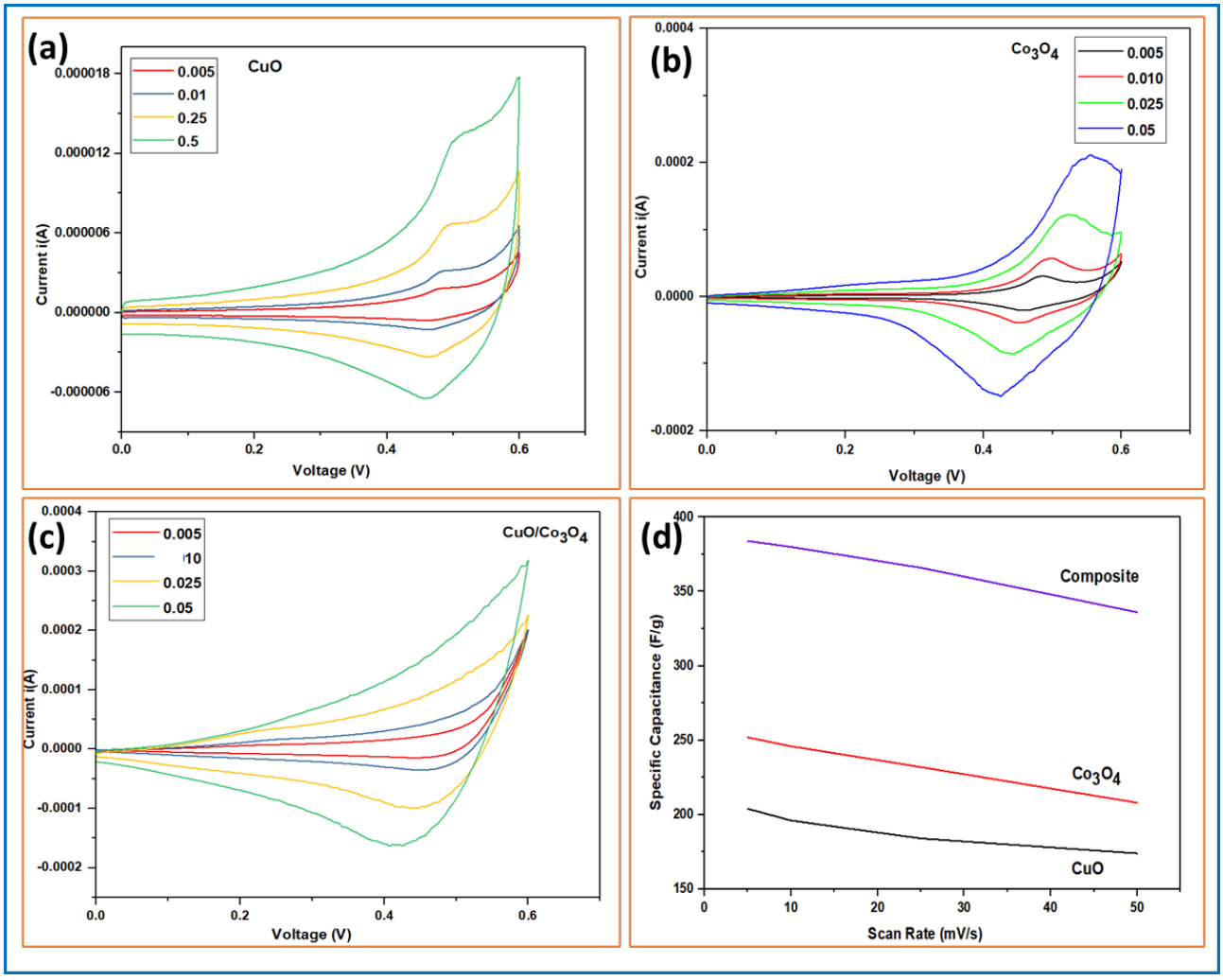

Figure 6. CV analysis of (a) CuO nanoparticle, (b) Co_3O_4 nanoparticle, (c) CuO/Co_3O_4 composite, (d) Specific Capacitance of synthesized nanomaterials at various scan rates.

Table 1. The specific capacitance decreases with increasing scan rates, which is a typical behaviour for supercapacitor materials. At lower scan rates, the ions have sufficient time to diffuse into the deeper active sites of the electrode material, resulting in higher capacitance values. Conversely, at higher scan rates, the ion diffusion is limited to the surface of the electrode material, leading to a decrease in capacitance. In addition, with increasing in scan rate (5, 10, 25, and 50 mV/s) the capacitance values decrease due to the inability of electrolyte ions to intercalate with the electrode active materials at higher scan rates. The new data underscore the hybrid nanoparticles' superior rate capability compared to the individual oxides, maintaining higher capacitance retention at elevated scan rates. This characteristic is crucial for practical applications where fast charge-discharge cycles are required, such as in power backup systems and electric vehicles.

Our study contributes to this research landscape by synthesizing and characterizing CuO, Co_3O_4, and CuO-Co_3O_4 hybrid nanoparticles using a sol-gel method. By comparing our findings with existing literature, we highlight the unique aspects of our synthesized materials, such as their specific

Table 1. Specific capacitance at various scan rates.

Scan Rate (mV/s)	CuO Specific Capacitance (F/g)	Co_3O_4 Specific Capacitance (F/g)	CuO/Co_3O_4 Specific Capacitance (F/g)
5	204	252	384
10	196	246	380
25	184	232	366
50	174	208	336

morphology, phase purity, and electrochemical performance metrics. The inclusion of this comparison underscores the novelty of our study and positions it within the current research forefront on advanced materials for supercapacitor applications.

We recognize the importance of further optimizing the synthesis parameters to enhance the performance of the CuO, Co_3O_4, and hybrid nanoparticles. As part of our future research, we plan to conduct systematic studies to investigate the effects of varying precursor concentrations, pH levels, reaction temperatures, aging times, and calcination temperatures on the morphology, size, crystallinity, and functional properties of the nanoparticles and the electrochemical performance of these materials under different cycling conditions and with other advanced characterization techniques.

4. Conclusion

In summary, this research underscores the promise of CuO, Co_3O_4, and their hybrid nanoparticles synthesized through the sol-gel approach as effective materials for supercapacitors. The synthesis method demonstrated effectiveness and flexibility in controlling the shape, structure, and composition of the resulting nanoparticles. Through deliberate adjustments in synthesis variables such as precursor concentrations, reaction temperatures, and durations, we could fine-tune the characteristics of CuO, Co_3O_4, and CuO-Co_3O_4 hybrid nanoparticles. CuO nanoparticles displayed a specific capacitance of 204 F/g, while Co_3O_4 nanoparticles showed 252 F/g at a scan rate of 5 mV/s. Notably, the CuO-Co_3O_4 hybrid nanoparticles revealed a significant specific capacitance of 384 F/g, highlighting the advantageous combined effects of hybridization. These observed synergies in the hybrid nanoparticles offer improved energy storage capabilities, positioning them as promising options for the next generation of supercapacitor technologies. This study contributes valuable insights into the manufacturing and electrochemical performance of nanomaterials based on transition metal oxides, thus advancing the field of energy storage technologies. In conclusion, the synthesis and characterization of CuO, Co_3O_4, and CuO-Co_3O_4 hybrid nanoparticles have demonstrated their significant potential for high-performance supercapacitors. Moving forward continued research efforts focused on optimization, advanced characterization, and exploring diverse applications will be crucial in harnessing the full capabilities of these nanomaterials for future energy storage technologies.

Authors Contributions

Study conception and design: Damodaram Vandana Reddy, Chindukuri Maneesha; Data collection and editing manuscript: Tumma Bala Narsaiah, Data collection and Draft manuscript preparation: Lakshmana Naik Ramavathu.

Availability of Data and Materials

The data that support the findings of this study are available from the corresponding author upon reasonable request.

Conflict of Interests

The authors declare that they have no known competing financial interests or personal relationships that could have appeared to influence the work reported in this paper.

References

[1] A.G. Olabi, M.A. Abdelkareem, T. Wilberforce, A. Alkhalidi, T. Salameh, A.G. Abo-Khalil, M. Mutasim Hassan, and E. Taha Sayed. Battery electric vehicles: Progress, power electronic converters, strength (S), weakness (W), opportunity (O), and threats (T). *Int. J. Thermofl.*, 16:100212, 2022. DOI: https://doi.org/10.1016/j.ijft.2022.100212.

[2] J. Feng, X. Yuan, L. Hu, G. Xie, Z. Zhang, X. Li, J. Hu, C. Wang, and H. Wang. A comprehensive review of energy storage technology development and application for pure electric vehicles. *J. Energy Stor.*, 86:111159, 2024. DOI: https://doi.org/10.1016/j.est.2024.111159.

[3] K. Swagatika, B. Kumar Jena, and S. Basu. Advances in electrochemical energy storage device: Supercapacitor. *Energy Stor.*, page 119–147, 2021. DOI: https://doi.org/10.1002/9781119555599.ch4.

[4] K.O. Oyedotun, J.O. Ighalo, J.F. Amaku, C. Olisah, A.O. Adeola, K.O. Iwuozor, K.G. Akpomie, J. Conradie, and K.A. Adegoke. Advances in supercapacitor development: Materials, processes, and applications. *J. Elect. Mater.*, 52:96–129, 2023. DOI: https://doi.org/10.1007/s11664-022-09987-9.

[5] S.A. Delbari, L. Saleh Ghadimi, R. Hadi, S. Farhoudian, M. Nedaei, A. Babapoor, and A. Sabahi Namini. Transition metal oxide-based electrode materials for flexible supercapacitors: A review. *J. Alloys and Comp.*, 857:158281, 2021. DOI: https://doi.org/10.1016/j.jallcom.2020.158281.

[6] L. Naik, R.T. Bala Narsaiah, C.R. Ravikumar, A. Naveen Kumar, K. Vinutha, A.A. Jahagirdar, and H.C. Ananda Murthy. Synthesis and characterization of nickel cobalt vanadate ($NiCo_2V_2O_8$) nanostructures: photocatalytic and supercapacitor applications. *Asian J. Chem.*, 33:2831–2838, 2021. DOI: https://doi.org/10.14233/ajchem.2021.23416.

[7] X. Yu, Y. Wang, J. Zhang, J. Liu, A. Wang, and L. Ding. Recent development of copper based nanozymes for biomedical applications. *Adv. Healthcare Mater.*, 13:2302023, 2024. DOI: https://doi.org/10.1002/adhm.202302023.

[8] W. Kang, R. Wei, H. Yin, D. Li, Z. Chen, Q. Huang, P. Zhang, H. Jing, X. Wang, and C. Li. Unraveling sequential oxidation kinetics and determining roles of multi-cobalt active sites on Co_3O_4 catalyst for water oxidation. *J. Am. Chem. Soc.*, 145:3470–3477, 2023. DOI: https://doi.org/10.1021/jacs.2c11508.

[9] M. Sajid, W. Qayyum, A. Farhan, M.A. Qamar, and H. Nawaz. Progress in the development of copper oxide-based materials for electrochemical water splitting. *Int. J. Hydrogen Energy*, 62:209–227, 2024. DOI: https://doi.org/10.1016/j.ijhydene.2024.02.377.

[10] B. Rezaei, P. Yari, S.M. Sanders, H. Wang, V.K. Chugh, S. Liang, S. Mostufa, K. Xu, J.P. Wang, J. Gómez Pastora, and K. Wu. Magnetic nanoparticles: A review on synthesis, characterization, functionalization, and biomedical applications. *Small*, 20:2304848, 2024. DOI: https://doi.org/10.1002/smll.202304848.

[11] M. Khalaj, Z. Zarabi Golkhatmi, and A. Sedghi. High-performance supercapacitor electrode materials based on chemical co-precipitation synthesis of nickel oxide (NiO)/cobalt oxide (Co_3O_4)-intercalated graphene nanosheets binary nanocomposites. *Diamond and Related Mater.*, 114:108313, 2021. DOI: https://doi.org/10.1016/j.diamond.2021.108313.

[12] A. Bahari, S. Ahmady-Asbchin, M. Naeij, A. Farhadikoutenaei, and A. Al-Jilef. Green synthesis and study of structural properties of copper nanocrystallites from hawthorn plant extract and study of its antibacterial activities. *Int. J. Nano Dimens.*, 14:138–144, 2023. DOI: https://doi.org/10.22034/IJND.2023.1977078.2199.

[13] J.M. Xu, A.L. Yan, X.C. Wang, B.Q. Wang, and J.P. Cheng. A review of cobalt monoxide and its composites for supercapacitors. *Ceram. Int.*, 47:22229–22239, 2021. DOI: https://doi.org/10.1016/j.ceramint.2021.04.262.

[14] C. Zhang, C. Jialian, C. Weixi, L. Jinling, and C. Denglong. Hydrothermal synthesis of Cu_2O/CuO/hierarchical porous N-doped activated carbon with exceptional electrochemical performance. *J. Energy Stor.*, 60:106600, 2023. DOI: https://doi.org/10.1016/j.est.2022.106600.

[15] R. Naik, T. Lakshmana, B. Narsaiah, P. Justin, A. Naveen Kumar, M.N. Somashekar, N. Raghavendra, C.R. Ravikumar, A. Ahmad Khan, and M.S. Santosh. Hydrothermally synthesized cobalt vanadate nanoparticles for photocatalytic degradation of fast orange red dye and supercapacitor applications. *Mater. Sci. Eng. B*, 298:116861, 2023. DOI: https://doi.org/10.1016/j.mseb.2023.116861.

[16] W.H. Low, S.K. Poi, S.L. Siew, W.S. Chiu, and R.E. Ejikeme. Recent development of mixed transition metal oxide and graphene/mixed transition metal oxide based hybrid nanostructures for advanced supercapacitors. *J. Alloys Comp.*, 775:1324–1356, 2019. DOI: https://doi.org/10.1016/j.jallcom.2018.10.102.

[17] Deka S. Nanostructured mixed transition metal oxide spinels for supercapacitor applications. *Dalton Trans.*, 52:839–856, 2023. DOI: https://doi.org/10.1039/D2DT02733J.

[18] K. Athira, S. Dhanapandian, S. Suthakaran, and A. Manikandan. Facile hydrothermally grown CuO/Co_3O_4 nanocomposite as an effective electrode material for enhanced supercapacitor applications. *J. Mater. Sci: Mater. Elect.*, 35:268–275, 2024. DOI: https://doi.org/10.1007/s10854-024-12022-8.

[19] L. Congcong, L. Lingran, Y. Yang, Y. Ma, L. Qiao, and M. Zhu. Recent progress in Co_3O_4 based nanomaterials for supercapacitors. *Chem. Nano Mat.*, 9:202200537, 2023. DOI: https://doi.org/10.1002/cnma.202200537.

[20] N. Parveen, S.A. Ansari, B.T. Al-Abawi, and M.O. Ansari. Fabrication of binder-free hierarchical three dimensional NiO nanoflakes@carbon nanofibers for superior symmetric supercapacitor application. *J. Energy Stor.*, 55:105619, 2022. DOI: https://doi.org/10.1016/j.est.2022.105619.

[21] M.Z. Ansari, S.A. Ansari, and S.H. Kim. Fundamentals and recent progress of Sn-based electrode materials for supercapacitors: A comprehensive review. *J. Energy Stor.*, 53:105187, 2022. DOI: https://doi.org/10.1016/j.est.2022.105187.

[22] S.A. Ansari, N. Parveen, G.M. Alsulaim, A.A. Ansari, S.A. Alsharif, K.M. Alnahdi, and V.R.M. Reddy. Emerging NiO–rGO nanohybrids for antibiotic pollutant degradation under visible-light irradiation. *Surf. Interf.*, 40:103078, 2023. DOI: https://doi.org/10.1016/j.surfin.2023.103078.

[23] S.S. Shah, F. Niaz, M.A. Ehsan, Das H. Tanaya, M. Younas, A. Sohail Khan, H. Ur Rahman, S.M. A. Nayem, M. Oyama, and M.D. Abdul Aziz. Advanced strategies in electrode engineering and nanomaterial modifications for supercapacitor performance enhancement: A comprehensive review. *J. Energy Stor.*, 79:110152, 2024. DOI: https://doi.org/10.1016/j.est.2023.110152.

[24] N. Parveen, G.M. Alsulaim, S.A. Alsharif, H.H. Almutairi, H.A. Alali, S.A. Ansari, and M.M. Ahmad. Renewable biopolymer-derived carbon–nickel oxide nanocomposite as an emerging electrode material for energy storage applications. *J. Sci: Adv. Mater. Dev.*, 8:100591, 2023. DOI: https://doi.org/10.1016/j.jsamd.2023.100591.

[25] H.I. Alrayzan, S.A. Ansari, and N. Parveen. Fabrication of asymmetric supercapacitor device based on nickel hydroxide electrode-graphene assembly. *J. Nanoelect. Optoelect.*, 17:536–543, 2022. DOI: https://doi.org/10.1166/jno.2022.3246.

[26] X. Lijing, F. Su, L. Xie, X. Guo, Z. Wang, Q. Kong, and G. Sun. Effect of pore structure and doping species on charge storage mechanisms in porous carbon-based supercapacitors. *Mater. Chem. Front.*, 9:2610–2634, 2020. DOI: https://doi.org/10.1039/D0QM00180E.

[27] S. Nilimapriyadarsini, B. Saravanakumar, M. Kundu, L. Schmidt-Mende, and A. Ramadoss. Recent trends in template assisted 3D porous materials for electrochemical supercapacitors. *J. Mater. Chem. A*, 9:25286–25324, 2021. DOI: https://doi.org/10.1039/D1TA06122D.

[28] T. Schoetz, L.W. Gordon, S. Ivanov, A. Bund, D. Mandler, and R.J. Messinger. Disentangling faradaic, pseudocapacitive, and capacitive charge storage: A tutorial for the characterization of batteries, supercapacitors, and hybrid systems. *Electrochem. Acta*, 412:140072, 2022. DOI: https://doi.org/10.1016/j.electacta.2022.140072.

[29] M. Dai, H. Liu, D. Zhao, X. Zhu, A. Umar, H. Algarni, and X. Wu. Ni foam substrates modified with a $ZnCo_2O_4$ nanowire-coated $Ni(OH)_2$ nanosheet electrode for hybrid capacitors and electrocatalysts. *ACS Appl. Nano Mater.*, 4:5461–5468, 2021. DOI: https://doi.org/10.1021/acsanm.1c00825.

[30] T. Xia, D. Zhao, Q. Xia, A. Umar, and X. Wu. Realizing high performance flexible supercapacitors by electrode modification. *RSC Adv.*, 11:39045–39050, 2021. DOI: https://doi.org/10.1039/D1RA07880A.

[31] H.R. Lee, M.S. Akhtar, A. Umar, A.A. Ibrahim, S. Baskoutas, and O.B. Yang. 2D $NiMoO_4$ nanowalls directly grown on Ni foam for the asymmetric electrochemical supercapacitors. *Chem. Phys. Impact*, 8:100406, 2024. DOI: https://doi.org/10.1016/j.chphi.2023.100406.

[32] W. Yared, N. Palaniyandy, V. Srinivasu Vallabhapurapu, and B.B. Mamba. Nanotechnology in advanced 2D and 3D nanostructured transition metal oxide based flexible supercapacitors: A Review. *Chem. Electro. Chem.*, 10:202300463, 2023. DOI: https://doi.org/10.1002/celc.202300463.

[33] N.U. Jude, R.M. Obodo, C.N. Agnes, C.N. Assumpta, M.E. Paul, and I.E. Fabian. *Recent advances in usage of cobalt oxide nanomaterials as electrode material for supercapacitors.* 2021. eBook ISBN: 9781003145585.

[34] A. Umar, I. Jung, A.A. Ibrahim, M.S. Akhtar, S.A. Kumar, M.A. Alhamami, and S. Baskoutas. Porous Mn_2O_3 nanorods-based electrode for high-performance electrochemical supercapacitor. *J. Energy Storage*, 81:110305, 2024. DOI: https://doi.org/10.1016/j.est.2023.110305.

[35] S.A. Ansari, N. Parveen, M.A.S. Al-Othoum, and M.O. Ansari. Development of binder free interconnected 3D flower of $NiZn_2O_4$ as an advanced electrode materials for supercapacitor applications. *Crystals*, 12:14–19, 2021. DOI: https://doi.org/10.3390/cryst12010014.

[36] N. Parveen, M.O. Ansari, S.A. Ansari, and P. Kumar. Nanostructured titanium nitride and its composites as high-performance supercapacitor electrode material. *Nanomater.*, 13:105–109, 2022. DOI: https://doi.org/10.3390/nano13010105.

[37] N.M. Tatiana, R. Kalusulingam, S. Tatiana, and A. Mikhailova. Sol-gel materials for electrochemical applications: Recent advances. *Coatings*, 12:1625–1629, 2022. DOI: https://doi.org/10.3390/coatings12111625.

[38] S. Sapan Kumar, U.C. Barman, M.S. Manir, P. Mondal, S. Dutta, M. Paul, M.A.M. Chowdhury, and M.A. Hakim. X-ray peak profile analysis of pure and Dy-doped α-MoO_3 nanobelts using Debye-Scherrer, Williamson-Hall and Halder-Wagner methods. *Adv. Natural Sci: Nanosc. Nanotechnol.*, 11:025004, 2020. DOI: https://doi.org/10.1088/2043-6254/ab8732.

[39] M. Nasrallah, H.A. Saleh, and A.M. Abdel-Karim. Exploring the optical and electrical characteristics of $CuO/CuCo_2O_4$ composites. *Sci. Sinter.*, 54:3–7, 2022. DOI: https://doi.org/10.2298/SOS2203265D.

[40] V. Monu, M. Mitan, H. Kim, and D. Vaya. Efficient photocatalytic degradation of Malachite green dye using facilely synthesized cobalt oxide nanomaterials using citric acid and oleic acid. *J. Phys. Chem. Solids*, 155:110125, 2021. DOI: https://doi.org/10.1016/j.jpcs.2021.110125.

[41] S. El-Sayed and A.M. El Sayed. Preparation and characterization of CuO/Co_3O_4/poly (methyl methacrylate) nanocomposites for optical and dielectric applications. *J. Mater. Sci: Mater. Electron.*, 32:13719–13737, 2021. DOI: https://doi.org/10.1007/s10854-021-05949-9.

[42] K. Niraj, V. Gajraj, R. Rameshbabu, R.V. Mangalaraja, N.C. Joshi, and N. Priyadarshi. Redox additive electrolyte assisted promising pseudocapacitance from strictly 1D and 2D blended structures of MnO_2/rGO. *Mater. Character.*, 189:111991, 2022. DOI: https://doi.org/10.1016/j.matchar.2022.111991.

[43] R. Lakshmana Naik, S.R. Harapanahalli, N. Pernapati, and B. Tumma. Synthesis and characterization of Nickel Metavanadate. *Int. J. Nano Dimens.*, 12:411–421, 2021. DOI: https://doi.org/10.22034/IJND.2021.682472.